

SCIENTIFIC REPORTS



OPEN

Spatial Heterogeneity of SOM Concentrations Associated with White-rot Versus Brown-rot Wood Decay

Zhen Bai, Qiang Ma, Yucheng Dai, Haisheng Yuan, Ji Ye & Wantai Yu

White- and brown-rot fungal decay via distinct pathways imparts characteristic molecular imprints on decomposing wood. However, the effect that a specific wood-rotting type of fungus has on proximal soil organic matter (SOM) accumulation remains unexplored. We investigated the potential influence of white- and brown-rot fungi-decayed *Abies nephrolepis* logs on forest SOM stocks (i.e., soil total carbon (C) and nitrogen (N)) and the concentrations of amino sugars (microbial necromass) at different depths and horizontal distances from decaying woody debris. The brown-rot fungal wood decay resulted in higher concentrations of soil C and N and a greater increase in microbial necromass (i.e., 1.3- to 1.7-fold greater) than the white-rot fungal wood decay. The white-rot sets were accompanied by significant differences in the proportions of the bacterial residue index (muramic acid%) with soil depth; however, the brown-rot-associated soils showed complementary shifts, primarily in fungal necromass, across horizontal distances. Soil C and N concentrations were significantly correlated with fungal rather than bacterial necromass in the brown-rot systems. Our findings confirmed that the brown-rot fungi-dominated degradation of lignocellulosic residues resulted in a greater SOM buildup than the white-rot fungi-dominated degradation.

Nearly one-quarter of Earth's land surface is covered by forests in which the decomposition of woody debris continuously recycles plant biomass; consequently, varying amounts of leachate and particulate matter enter the soil system over a period of decades^{1–4}. Soil carbon (C) and nitrogen (N) concentrations are greatly influenced by the initial composition of litter (e.g., woody debris) when soil mineralogy and texture are similar^{1,5,6}. Moreover, soil C and N concentrations can also be affected by the pathways undertaken and the complex compounds produced by the degradation of specific lignocellulosic residues^{7–9}, as well as the soil microbes that are present or active in the working systems^{10,11}.

Wood residues are primarily composed of lignin, cellulose and hemicellulose^{12,13}, and wood-rotting fungi dominate the decomposition process^{14–16}. For instance, white-rot fungi can either degrade lignin and leave relatively high levels of white-colored cellulose or hemicellulose along with degraded lignin fragments; alternatively, these fungi can degrade lignin and cellulose simultaneously^{7,14,17}. Although brown-rot fungi can promote the extensive decay of cellulose and hemicellulose through both enzymatic and non-enzymatic mechanisms, the lack of lignin-degrading extracellular phenoloxidases may lead to the accumulation of depolymerized and demethylated brown-colored lignin in litter and surface soils^{15,18–21}. During the decomposition processes dominated by white- or brown-rot fungi, soluble wood decay products can be leached into soils and adsorbed onto the hydroxide surfaces of cations in the soil matrix, thereby affecting the formation and protection of soil organic matter (SOM)^{1,18,22}. This process can evolve in a cascading cycle of abiotic adsorption and microbial uptake that can be described in terms of a soil dynamic continuum²³.

The effects of the soil microbial community on the leached wood decay products determine SOM storage because distinct microbial compositions and byproducts have different effects on the formation and stabilization of organic substances. For instance, high fungal/bacterial ratios may be associated with increased C sequestration in soils^{10,11}. In addition, the soil microbial necromass can underpin the formation and stabilization of long-lived SOM^{24–27}, which is particularly pertinent when mineral and particle sorptive interactions favor matrix protection

Institute of Applied Ecology, Chinese Academy of Sciences, Shenyang, 110016, China. Correspondence and requests for materials should be addressed to Q.M. (email: qma@iae.ac.cn) or W.Y. (email: wtyu@iae.ac.cn)

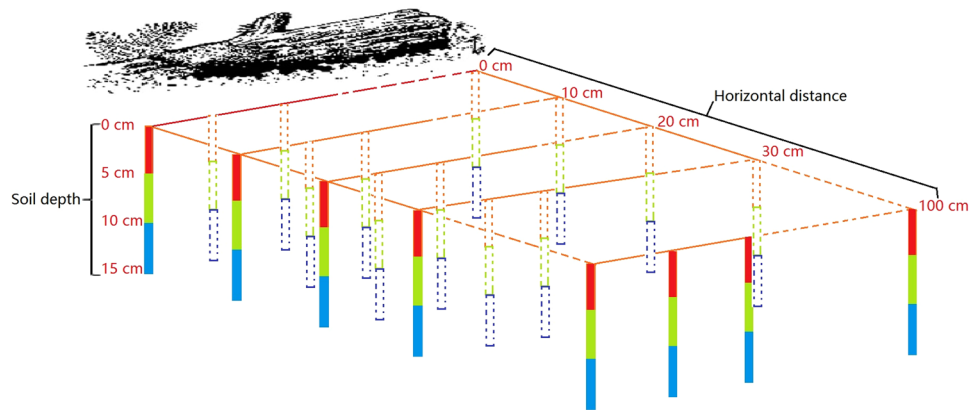


Figure 1. Illustration of the sampling design for soil samples around woody debris. Soil depth increments are 0–5 cm (D_{0-5} , red column), 5–10 cm (D_{5-10} , green column) and 10–15 cm (D_{10-15} , blue column). Separate horizontal distances radiate perpendicularly from woody debris at 0 cm (i.e., directly beneath the woody debris, Zone H_0), 10 cm (Zone H_{10}), 20 cm (Zone H_{20}), 30 cm (Zone H_{30}) and 100 cm (Zone H_{100}).

and the recalcitrance of certain organic products of secondary microbial synthesis^{27–29}. By contrast, dissolved decay products may also have the potential to facilitate the loss of previously stable soil C through microbial excavation³⁰, whereby soil microbes increase their rates of decomposition of original soil C with the introduction of an additional C source because of changes in substrate preference, activity, or community structure^{31–33} or the selective liberation of mineral- or physically-protected C³⁴.

A considerable knowledge gap exists with regard to the linkage between the specific lignocellulosic residues of wood-decaying processes (e.g., white- vs. brown-rot) and proximal belowground microbially-mediated C and N cycling. The effects of surficial wood decay products on microbially-mediated SOM accumulation are difficult to assess quantitatively using most of the currently available techniques, such as culture-dependent methods, pyrosequencing-based approaches for nucleic acid analysis, phospholipid fatty acid analyses, substrate utilization capacities, and state-of-the-art metaproteomics^{35–40}. However, microbially-mediated SOM formation induced by wood decay products can be estimated based on amino sugars, which are important cell wall components that can persist for several decades after the lysis of viable microbial cells^{41,42}. Three amino sugars—glucosamine (GluN), galactosamine (GalN) and muramic acid (MurN)—and their ratios have been quantified and extensively used to indicate specific microbial necromass contents and community structure^{43–45}. Fungal cell walls contain a polymer of N-acetylglucosamine, whereas the peptidoglycan of bacterial cell walls contains both N-acetylglucosamine and N-acetylmuramic acid^{44,46,47}. Therefore, MurN is usually used to indicate bacterial residues, and GluN is generally considered a primary biomarker of both fungal and bacterial necromass^{43,44,48}. Furthermore, variations in the GluN/GalN and GluN/MurN and GalN/MurN ratios may be closely correlated with different fungal or bacterial predominance^{43,44,49}. Thus, long-lived amino sugars can be a proxy of microbial necromass abundance and composition, which are directly linked to SOM storage during wood decay.

As described above, the brown- and white-rot fungal decay pathways progressively alter the lignocellulose composition of woody debris but with different chemical outcomes for both lignin constituents and structural carbohydrates. White rot degrades lignin, leaving cellulose or hemicellulose largely intact, whereas brown rot, which decomposes cellulose or hemicellulose, results in highly concentrated lignin components. The products, i.e. leachate⁵⁰ or particulate matter⁵¹ resulting from these two decomposition pathways, can be expected to exert distinct effects on soil microbial metabolism, necromass accumulation and overall soil C and N dynamics proximal to long-lived decay sources. Understanding the effects of each wood-rotting type of fungus on soil nutrient cycles can provide quantitative information on C and N allocation, residence, and stocks in forest ecosystems. To address this issue, we analyzed the concentrations of C and N and the composition of amino sugars in soil immediately below (0–15 cm) and laterally adjacent to (0–1 m) logs in advanced stages of either brown- or white-rot decay (Fig. 1) in a mixed-species forest within the Changbai Mountain Nature Reserve (CBMNR) of northeastern China.

Results and Discussion

Spatial heterogeneity of C and N and microbial necromass caused by wood decay. The soil total C, total N and amino sugar concentrations increased in regions proximal to woody debris in the current study. For instance, the soil C concentrations were lower in Zone H_{100} (5.8%) than in Zone H_0 (8.5%), and the soil N concentrations varied little from Zone H_0 to Zone H_{30} (~0.5%) but were lower in Zone H_{100} (0.4%) (Table 1, Fig. 2a). Compared with the surface soil (D_{0-5}), the subsurface soil C and N concentrations decreased by 53.2–67.7% and 50.0–62.5%, respectively, at depths of 5–10 (D_{5-10}) and 10–15 cm (D_{10-15}) ($p < 0.05$) (Table 1, Fig. 2a). Consistently, the fungal and bacterial necromass C concentrations were higher (ca. 50%) in the surface than in the subsurface soils ($p < 0.05$). A horizontal stratification effect was detected for fungal residues between Zones H_{10} and H_{100} (Table 1). In a previous study, the soil beneath woody debris in *Eucalyptus* woodlands in southeastern Australia contained higher C and N concentrations than soil located 80 cm horizontally from the woody debris⁵². Additionally, as a result of well-decayed woody debris, surface soils have lower pH and higher exchangeable

Variables		Rot types	Horizontal distances	Soil depths
C (%)	Rank	white-rot(4.8) < brown-rot(11.2)	H ₀ (8.5) ≈ H ₁₀ (8.1) ≈ H ₂₀ (7.4) ≈ H ₃₀ (7.2) ≈ H ₁₀₀ (5.8)	D ₀₋₅ (12.4) > D ₅₋₁₀ (5.8) ≈ D ₁₀₋₁₅ (4.0)
	H-value	(25.3) ^{***}	(2.7)	(33.6) ^{***}
N (%)	Rank	white-rot(0.3) < brown-rot(0.8)	H ₀ (0.5) ≈ H ₁₀ (0.5) ≈ H ₂₀ (0.5) ≈ H ₃₀ (0.5) ≈ H ₁₀₀ (0.4)	D ₀₋₅ (0.8) > D ₅₋₁₀ (0.4) ≈ D ₁₀₋₁₅ (0.3)
	H-value	(30.7) ^{***}	(1.8)	(31.5) ^{***}
C/N	Rank	white-rot(13.7) ≈ brown-rot(14.3)	H ₀ (15.6) ≈ H ₁₀ (14.4) ≈ H ₂₀ (13.9) ≈ H ₃₀ (13.0) ≈ H ₁₀₀ (12.8); H ₀ > H ₃₀ ^a	D ₀₋₅ (15.5) > D ₅₋₁₀ (13.6) ≈ D ₁₀₋₁₅ (12.8)
	H-value	(1.6)	(10.1) [*]	(22.8) ^{***}
Fun C (mg g ⁻¹)	Rank	white-rot(19.7) < brown-rot(52.7)	H ₀ (35.1) ≈ H ₁₀ (35.1) ≈ H ₂₀ (34.6) ≈ H ₃₀ (33.1) ≈ H ₁₀₀ (27.3)	D ₀₋₅ (52.9) > D ₅₋₁₀ (28.5) ≈ D ₁₀₋₁₅ (18.9)
	H-value	(34.2) ^{***}	(1.8)	(24.8) ^{***}
Bac C (mg g ⁻¹)	Rank	white-rot(3.7) < brown-rot(10.0)	H ₀ (6.6) ≈ H ₁₀ (5.8) ≈ H ₂₀ (6.0) ≈ H ₃₀ (7.4) ≈ H ₁₀₀ (5.5)	D ₀₋₅ (9.2) > D ₅₋₁₀ (5.4) ≈ D ₁₀₋₁₅ (4.4)
	H-value	(32.0) ^{***}	(1.3)	(18.6) ^{***}
Fun/Bac C	Rank	white-rot(5.3) ≈ brown-rot(6.2)	H ₀ (5.7) ≈ H ₁₀ (6.1) ≈ H ₂₀ (6.1) ≈ H ₃₀ (5.2) ≈ H ₁₀₀ (5.4)	D ₀₋₅ (6.8) ≈ D ₅₋₁₀ (5.8) ≈ D ₁₀₋₁₅ (4.6); D ₀₋₅ > D ₁₀₋₁₅
	H-value	(2.1)	(3.4)	(6.3) [*]

Table 1. Analysis of variance results of the effects of rot types, horizontal distances and soil depths on soil C and N and microbial necromass. Note: Mean values of specific treatment are presented in parentheses. Variables include soil carbon (C) and nitrogen (N), fungal necromass carbon (Fun C) and bacterial necromass carbon (Bac C). White- and brown-rot fungi are shortened to white- and brown-rot, respectively. Horizontal distances are indicated as H₀ (0 cm), H₁₀ (10 cm), H₂₀ (20 cm), H₃₀ (30 cm) and H₁₀₀ (100 cm). Soil depths are indicated as D₀₋₅ (0–5 cm); D₅₋₁₀ (5–10 cm) and D₁₀₋₁₅ (10–15 cm). Differences between factor levels were detected using Kruskal–Wallis test. ^{***} $p < 0.001$; ^{**} $p < 0.01$; ^{*} $p < 0.05$; ^a $p < 0.1$.

acidity (especially those associated with brown-rot fungi, Supplementary Table S1), partly as a result of the accumulation of more polyphenols directly beneath decaying wood⁵³. Such large spatial heterogeneity of soil properties resulting from wood decay can be explained by the translocation of the soluble fractions of degraded wood products via water percolation into the soil^{1,54}. These transported components enrich C and N concentrations in SOM pools either through adsorption to soil particles or via immobilization in soil microbial community biomass^{5,6,53}.

The soil C/N ratios were higher at D₀₋₅ (15.5) than at D₅₋₁₀ (13.6) and D₁₀₋₁₅ (12.8) ($p < 0.05$) and decreased from Zone H₀ (15.6) to Zone H₁₀₀ (12.8) ($p < 0.1$) (Table 1, Fig. 2b). These C/N ratios are much lower than those in rotten wood^{51,55,56}. Similar relationships have been demonstrated for a Douglas-fir forest stand⁵⁷ in which the C/N ratios of mineral soil below woody debris were lower than those of any aboveground detrital component and decreased from 26 to 18 along the soil profile. The decline in the soil C/N ratio with increasing horizontal distance from woody debris is consistent with the results presented by Goldin and Hutchinson⁵², who found that soil C/N ratios were, on average, 15.1 at 0 cm and 13.1 at 80 cm from woody debris. Such plant-derived molecular imprints on soil C/N ratios—being much lower than and increasing closer to aboveground woody debris—are unequivocally a consequence of both the marked increase in N concentration during the process of litter decay and the highly concentrated C resources in woody debris^{6,58,59}. Increasing concentrations of N during wood-decaying processes are explained by N immobilization by directly contacted fungal hyphae and the interactions with diazotrophs^{57,60,61}. Simultaneously, highly enriched recalcitrant wood C compounds probably result in a constant C fraction in wood decay leachates^{59,62}.

Greater SOM buildup beneath the brown- compared with the white-rot sets. The concentrations of C, N and microbial necromass proxies were higher under the brown-rot decayed wood than under the white-rot decayed wood (Table 1, Supplementary Tables S2 and S3): (1) the C and N concentrations were approximately 1.3- and 1.7-fold higher, respectively ($p < 0.05$), and (2) the fungal and bacterial necromass C concentrations were approximately 1.7-fold higher ($p < 0.05$). Brown-rot woody debris contains high concentrations of soluble aromatic and phenolic compounds and metals²¹; its presence may thus promote chemical and physical protection of both itself and the existing SOM from degradation, consequently increasing the mean residence time of soil C and contributing to further SOM “stabilization” along a soil profile or at discrete distances from the woody debris^{1,8,15,18}. By contrast, white-rot fungi have aggressive enzyme systems for both hydrolytic and ligninolytic activities, which allow the complete decay and disruption of the structural and chemical components of cell walls^{17,63,64}. The soluble sugars and other rapidly metabolized components progressively released at low rates from white-rot woody debris are most likely available to nearby R-strategists, which promote the decomposition of extant SOM to acquire available N, leading to increased mineralization of the SOM pools^{65–67}. The negative relationships between the bacterial residue index (MurN) and lignin monomers V, S, and C (Table 2) might indicate a reduction in the bacterial growth caused by the acidic products released during the white-rot decay process. Such inhibition of bacterial growth induced by white-rot decay products was significantly reduced as lignin oxidation proceeded because lignin fragments Ac/Al (V) and C/V ratios, which increase with lignin oxidation and soil depth⁶⁸, were positively correlated with bacterial residue concentrations in this study (Table 2).

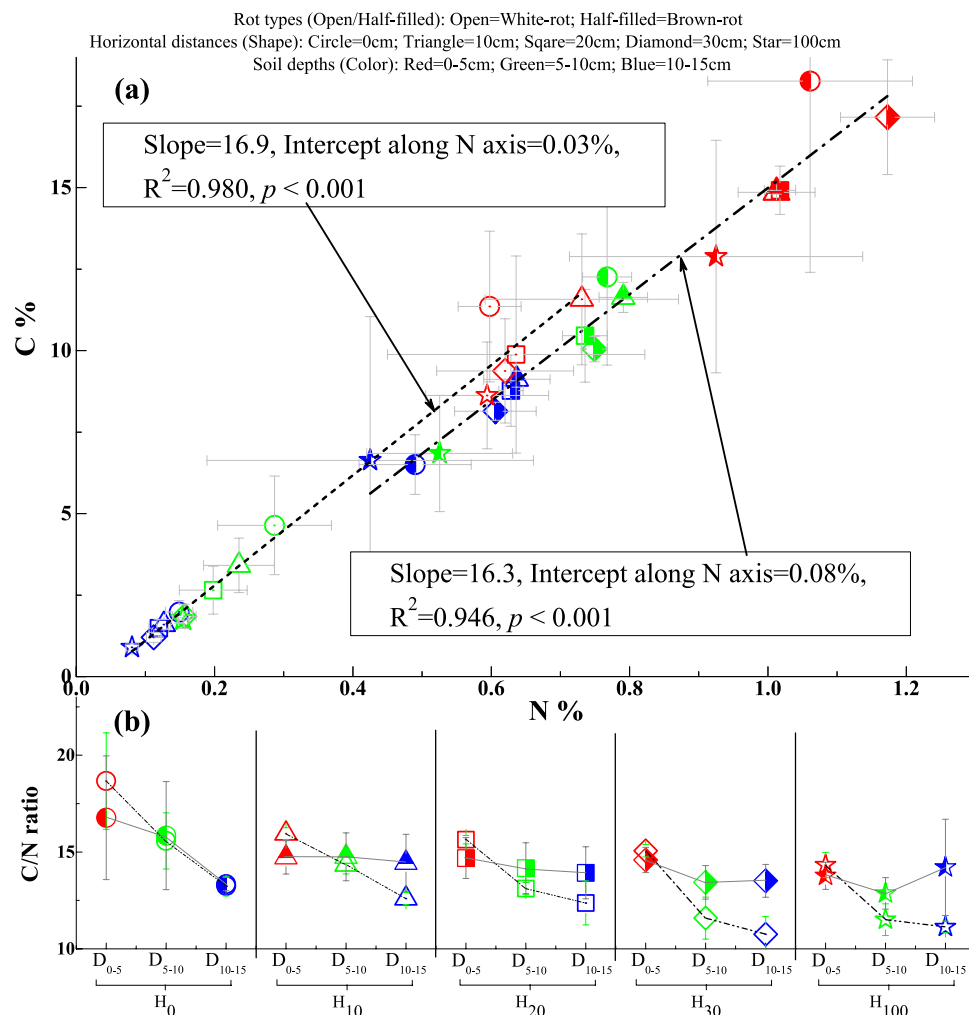


Figure 2. The C and N abundances and C/N ratios at three different soil depths from beneath the coarse woody debris to a perpendicular distance of 100 cm as a result of the brown- or white-rot fungi. **(a)** C and N concentrations and their relationships; **(b)** C/N ratios. Horizontal distances are separately indicated as H_0 (0 cm), H_{10} (10 cm), H_{20} (20 cm), H_{30} (30 cm) and H_{100} (100 cm). Soil depths are represented by D_{0-5} (0–5 cm), D_{5-10} (5–10 cm) and D_{10-15} (10–15 cm).

Amino sugars Lignin monomers	GluN ($\text{mg g}^{-1}\text{C}$)	GalN ($\text{mg g}^{-1}\text{C}$)	MurN ($\text{mg g}^{-1}\text{C}$)	Total amino sugars ($\text{mg g}^{-1}\text{C}$)
V ($\text{mg g}^{-1}\text{C}$)	−0.47 (−0.36)	−0.47 (−0.43)	−0.64 (−0.36)	−0.48 (−0.46)
S ($\text{mg g}^{-1}\text{C}$)	−0.43 (0.34)	−0.36 (0.03)	−0.61 (−0.13)	−0.43 (0.24)
C ($\text{mg g}^{-1}\text{C}$)	−0.41 (0.21)	−0.41 (−0.31)	−0.59 (−0.34)	−0.43 (−0.01)
S + V + C ($\text{mg g}^{-1}\text{C}$)	−0.53 (−0.23)	−0.52 (−0.41)	−0.73 (−0.38)	−0.54 (−0.36)
Ac/Al (V)	0.25 (−0.41)	0.19 (−0.20)	0.40 (0.09)	0.24 (−0.36)
Ac/Al (S)	−0.15 (0.09)	−0.11 (0.06)	−0.22 (−0.19)	−0.15 (0.07)
S/V	0.05 (0.16)	0.07 (0.50)	0.10 (0.45)	0.06 (0.36)
C/V	0.54 (0.32)	0.51 (0.33)	0.63 (0.39)	0.54 (0.39)

Table 2. Correlation between lignin monomers and amino sugars in white-rot (brown-rot) sets. Note: The vanillyl (V), syringyl (S) and cinnamyl (C) phenolic units separated using the cupric oxide (CuO) method were used as a measure of the lignin monomer concentrations in soil. The oxidation state of V or S lignin fragments is indicated as Ac/Al (i.e., the acid/aldehyde ratio). S/V indicates the syringyl/vanillyl ratio, and C/V indicates the cinnamyl/vanillyl ratio. Three amino sugars, namely glucosamine (GluN), galactosamine (GalN) and muramic acid (MurN), were quantified to reveal the soil microbial necromass composition. The values in the table are “r” values, i.e., the correlation between lignin monomers and amino sugars in the white-rot (brown-rot) sets. Significant values ($p < 0.05$) are indicated in boldface.

Horizontal distances (Shape): Circle=0cm; Triangle=10cm; Square=20cm; Diamond=30cm; Star=100cm

Soil depths (Color): Red=0-5cm; Green=5-10cm; Blue=10-15cm

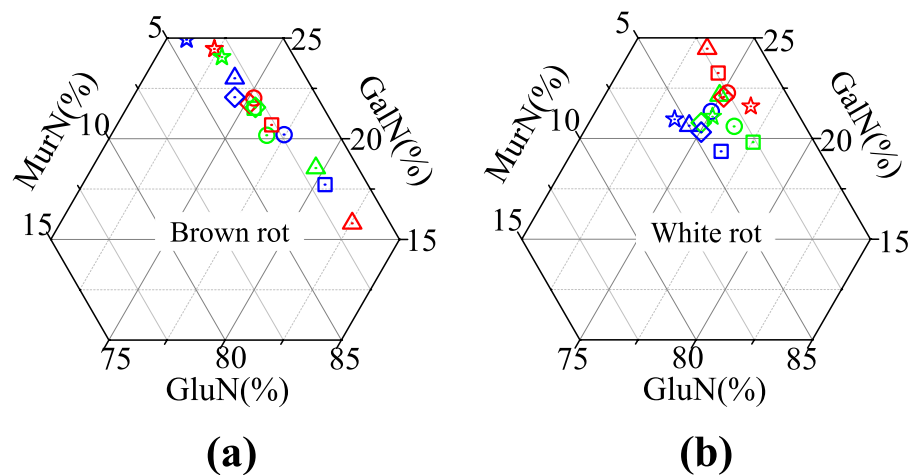


Figure 3. The ternary diagram of amino sugars at three different soil depths from beneath the coarse woody debris to a perpendicular distance of 100 cm. **(a)** The ternary diagram of amino sugar compositions associated with brown rot; **(b)** The ternary diagram of amino sugar compositions associated with white rot.

Moreover, brown-rot fungal growth, which selectively enriches lignin polymers that are bound to over 50% of wood N⁶⁹, most likely favors N condensation, whereas delignification with simultaneous N utilization by white-rot fungal growth is linked to low N concentration and availability in decayed woody debris^{70–72}. Furthermore, brown-rot woody residues are more likely to accumulate N compared with white-rot residues because brown-rot fungi can efficiently accelerate N₂ fixation^{61,73} and are therefore a more favorable ecological niche for mycorrhizal growth⁷⁴. These different mechanisms most likely resulted in the 0.05% higher N concentration in the brown- than in the white-rot-associated soil, which was evident in the comparison of the intercepts of the regression curves along the N% axis (i.e., if the C concentration equaled 0, the N concentration should be 0.08% for the brown-rot sets and 0.03% for the white-rot sets) (Fig. 2a). The values of these intercepts along the N% axis on average accounted for ca. 10% of the N concentrations in the brown- and white-rot-associated soils, as the mean N concentrations in these soils were 0.8% and 0.3% (Table 1), respectively.

Linkage of microbial necromass to C and N concentrations in soil. Using the ternary diagram of the relative abundances of three amino sugars, we classified the microbial necromass composition into two contrasting patterns between the brown- and white-rot-associated soils (Fig. 3). With respect to the soil amino sugar composition in the brown-rot sets (Fig. 3a), Zone H₁₀₀ displayed the highest GalN% but the lowest GluN% (i.e., primary fungal residue index). This was significantly distinct from Zones H₀ to H₃₀, in which the opposite trend was observed ($p < 0.05$, except for D_{10–15} in Zone H₁₀). By contrast, the ternary plot of amino sugar composition in the white-rot affected soils clearly revealed a significant shift in the MurN (bacterial residue index) proportion with soil depth (Fig. 3b), i.e., D_{0–5} < D_{5–10} < D_{10–15} ($p < 0.05$).

Acidic leachates from woody debris significantly decreased the pH of nearby surface mineral soils⁵³. Jiao *et al.*⁷⁵ reported that the pH values (soil: water = 1: 2.5) of the same rot-associated soils as in this study varied from 3.8 to 5.5 in the brown-rot sets and were lower than those in the white-rot sets (5.0–5.7) (Supplementary Table S1). Brown-rot fungi produce more oxalic acid and lignin phenolics, which result in lower pH and inhibit the activities of bacteria in brown- compared with white-rot systems^{65,76,77}. Additionally, white-rot fungi oxidize acidic products such as cellobionic acid and oxalic acid^{76,78}. These findings support (1) the significant correlations between the bacterial residue index (MurN) and lignin monomers and their ratios (Table 2, and (2) higher relative abundances of bacteria in the white- than brown-rot sets (Fig. 3). Fungal/bacterial ratios are positively correlated with the soil C/N ratios because bacteria require more N per unit of biomass C assimilation than fungi¹¹, and higher C assimilation efficiencies are correlated with larger proportions of fungi but not with larger proportions of bacteria^{79–82}. We observed that the C/N ratios decreased to a greater extent along soil profiles with increasing horizontal distance for the white- than for the brown-rot woody debris (Fig. 2b).

The fungal decomposer composition can change during plant residue degradation due to the changing quality of available decayed products⁸³. Over horizontal distances that radiate perpendicularly from woody debris, the translocated soluble wood products may present a gradient of substrate quality, i.e., soil closer to well-decayed woody debris has a higher concentration of recalcitrant substrates. Because the wood decay products exist longer in the brown- than in the white-rot systems, the spatial allocation of wood decay products should be more likely to occur in brown-rot systems. Consequently, it is reasonable to observe a fungal composition shift along horizontal distances in the brown-rot associated soils (Fig. 3a).

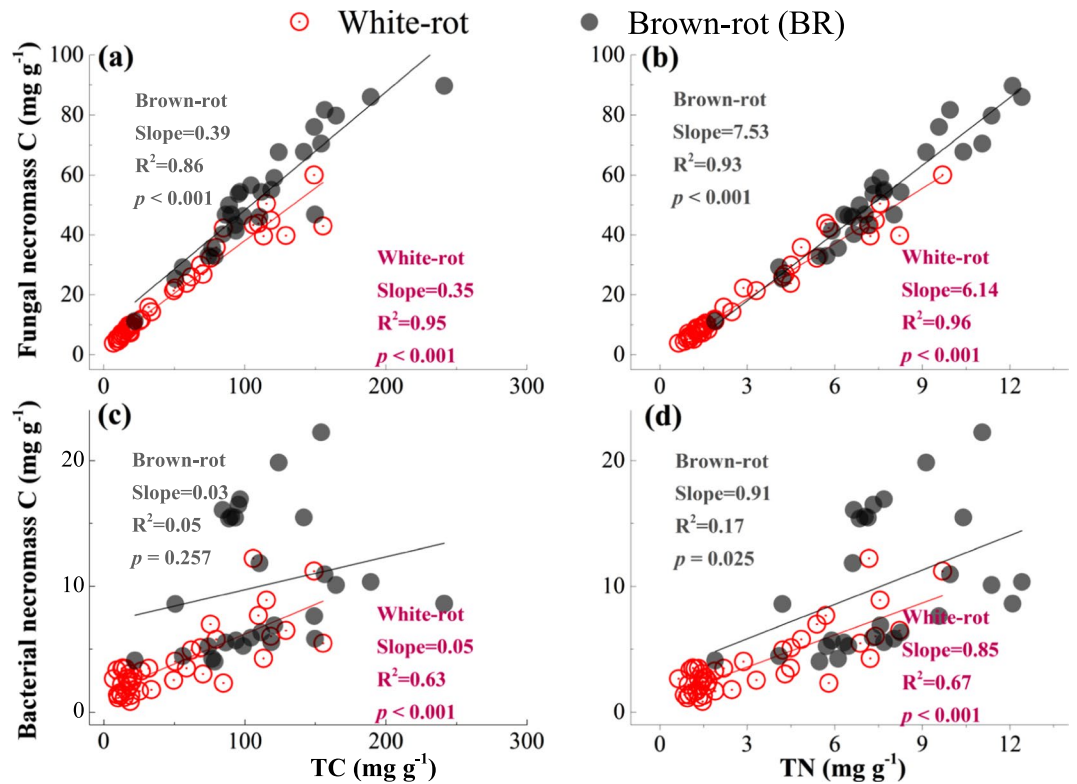


Figure 4. Correlations between microbial necromass and C and N concentrations at three different soil depths from beneath the coarse woody debris to a perpendicular distance of 100 cm. (a) Correlations between fungal residue C and C concentrations; (b) correlations between fungal residue C and N concentrations; (c) correlations between bacterial residue C and C concentrations; (d) correlations between bacterial residue C and N concentrations.

The slopes derived from the linear regressions of fungal necromass vs. C and N were greater in the brown- than in the white-rot sets (Fig. 4a and b). By contrast, the bacterial residues were not as well correlated with the soil C and N in the brown-rot-associated soils as they were in the white-rot-associated soils (Fig. 4c and d). These findings suggested that the bacterial residues in the brown-rot-associated soils were unresponsive in proportion to the increased fungal necromass C concentrations and therefore showed a lack of correlation with C and N concentrations, as observed for the white-rot-associated soils. The combination of higher C and N concentrations and a higher fraction of fungi in the brown- than in the white-rot systems (Table 1, Fig. 3) suggested that a microbial community with higher proportions of fungi under brown-rot woody debris preferentially maintained larger SOM stocks than the soil associated with white-rot woody debris in which bacterial residues were concentrated.

Materials and Methods

Description of the research area. The study site is in a mixed spruce, fir, birch, oak and aspen forest within the CBMNR (42°23'N, 128°05'E, 802 m a.s.l.). *Picea jezoensis* and *Abies nephrolepis* are the dominant tree species. Precipitation occurs primarily from June to September and averages 700 mm annually; the annual average temperature is 2.8 °C⁸⁴. The soil at the sampling site is an andosol that developed from volcanic ash⁸⁵.

Identification of decayed logs. We chose decayed logs (ca. 20 cm in diameter) that were in contact with soil and in the final decay stage⁶², which could be identified separately as decayed by brown-rot or white-rot fungi based on their fragmentation morphology^{2,16,55}. The brown-rot woody debris was characteristically “brittle and broke easily into cube-like pieces”, whereas the white-rot woody debris was “spongy with longitudinal fragmentation”⁶³ (see the pictures of woody debris in Supplementary Figure S4). The dominant fungal species responsible for the specific brown and white rot were identified based on their fruiting bodies. The white-rot-degraded logs of *Abies nephrolepis* were decomposed by the basidiomycete *Antrodia gypsea* (Yasuda) T. Hatt. & Ryvarden, which is a common fungus found primarily on gymnosperm wood that has a preference for *Abies*⁸⁶. The brown-rot-decayed logs of *Abies nephrolepis* were decomposed by *Fomitopsis pinicola* (Sw.) P. Karst, which is one of the most common wood decay basidiomycete fungi and is frequently found on both gymnosperms and angiosperms^{86,87}. The vanillyl (V), syringyl (S) and cinnamyl (C) phenolic units separated using the cupric oxide method⁸⁸ were used as measures of the concentrations of lignin monomers in the brown- and white-rot-associated soils. The results showed that much higher lignin concentrations occurred under the brown- than under the white-rot-associated soils (Supplementary Figure S5). For instance, at horizontal distances of 20 and 30 cm, the lignin concentrations were 54% and 72% greater, respectively, in the brown-rot-associated soils

than in the white-rot-associated soils; at a depth of 5–10 cm, the lignin concentrations were on average 318% higher under the brown- than under the white-rot sets. These findings are consistent with the fact that lignin is highly degraded and removed in white-rot sets, whereas brown-rot sets are characterized by the accumulation of depolymerized and demethylated lignin.

Sampling and processing of soil. Using a 2.5-cm-diameter auger, soil samples were collected on 3 September 2011 at three soil depths in five parallel zones that radiated perpendicularly from the chosen woody debris (Fig. 1). Soil was collected at depths of 0–5 (D_{0–5}, red column), 5–10 (D_{5–10}, green column) and 10–15 cm (D_{10–15}, blue column), and the horizontal distances from decomposing logs were 0 (i.e., directly beneath the woody debris, Zone H₀), 10 (Zone H₁₀), 20 (Zone H₂₀), 30 (Zone H₃₀) and 100 cm (Zone H₁₀₀). At least four soil cores were collected from each sampling zone. The width of each zone was less than 2.5 cm (diameter of the soil auger). Soil samples were collected on both sides of three logs for white rot and of two logs for brown rot, and soils were immediately homogenized thoroughly while moist (i.e., 5 rot sets × 5 horizontal zones × 3 depths = 75 composite samples). The soil samples were sieved through a 2-mm mesh to remove visible roots and rocks and were then air-dried and milled (<250 μm) to determine C, N, lignin and amino sugar concentrations.

Quantification of soil C, N, amino sugars and microbial necromass. Soil C and N concentrations were determined by dry combustion using an elemental analyzer (vario Macro cube; Elementar Analysensysteme GmbH, Hanau, Germany), and the C/N ratios are presented as mass ratios. Soil amino sugars, including GluN, GalN and MurN, were purified, derivatized and quantified according to Zhang and Amelung⁸⁹ with modifications by Liang *et al.*⁹⁰ In brief, the soil samples were digested by acid hydrolysis followed by iron and salt removal via precipitation and subsequent derivatization to aldonitrile derivatives. Gas chromatography separation and detection of derivatized amino sugars were performed using an HP-5 silica column (25 m × 0.32 mm × 0.25 μm) and flame ionization detector connected to an Agilent 6890 A GC (Agilent Tech. Co., USA).

Proxies for the relative necromass abundances of bacteria and fungi were determined using relative proportions of the extracted amino sugars^{91,92}. MurN primarily occurs in bacteria^{47,48}, whereas both fungal and bacterial cell walls contain GluN^{44,46}; a MurN:GluN ratio of 1:1 is the proportion found in bacterial cell walls^{91,93}. The microbial necromass C sources, i.e., fungal and bacterial residue C concentrations, were calculated as follows: fungal C mg g⁻¹ dry weight = 9 × 179.2 × (mol GluN – mol MurN), where 179.2 is the molecular weight of GluN and 9 is the conversion value of fungal GluN to fungal C; bacterial C mg g⁻¹ dry weight = 45 × MurN C, where 45 is the conversion index from MurN C to bacterial residue C^{91,92}.

Statistical analyses. Although this study only included two replicates for brown rot and three replicates for white rot, it was important to acquire predictions of soil organic C buildup and microbial necromass composition induced by specific rot decay (i.e., the brown vs. white rot) at our study site. Statistical analyses were performed (including 2 × brown-rot and 3 × white-rot sets) using Statistica 10 software (StatSoft, Inc., USA). The effects of soil depth, horizontal distance from decayed logs, and wood-rotting types of fungi were detected using a nonparametric test (the Kruskal-Wallis test) as the distribution of replicates is not homogenous between wood-rotting types. One-way analysis of variances (ANOVAs) were performed for each variable, followed by multiple comparisons between group levels (Kruskal-Wallis test, *p* < 0.05). Regression analysis and figure construction were performed using Origin 8.5 (OriginLab Corp., USA). A χ² test was used to assess the statistical significance between different subsamples in a ternary graph⁹⁴.

Data availability. The authors declare that the data in the current manuscript are available upon request.

Conclusions

Fungal wood decay resulted in high spatial heterogeneity of soil C and N and microbial necromass concentrations. The soil C and N concentrations of the brown-rot sets were higher than those of the white-rot sets, which suggested that brown rot contributed more to SOM buildup than white rot. A microbial community process, rather than a single-species dynamic, mediates plant-derived molecular contributions to SOM buildup. Because different microbial groups can form both unique and long-standing necromass components, amino sugar composition analysis can identify specific soil microbial footprints (i.e., the legacy of the microbial community) and provide a solid foundation to explain the microbial controls of and interactions within the soil nutrients stored during the process of fungal wood decay. Our findings of strong correlations between the fungal necromass and soil C and N concentrations in the brown-rot sets confirmed that higher proportions of fungi rather than bacteria contributed to a greater buildup of SOM. In future studies, which include increasing organic matter incorporation into soil fractions and mitigating CO₂ release in terrestrial ecosystems, the focus should be on the mechanisms of SOM stabilization and the genesis driven by specific types of wood decay (particularly for brown rot) in forests, in addition to the important contribution of microbial necromass in microbially-mediated soil processes.

References

1. Ganjegunte, G. K., Condon, L. M., Clinton, P. W., Davis, M. R. & Mahieu, N. Decomposition and nutrient release from radiata pine (*Pinus radiata*) coarse woody debris. *For. Ecol. Manag.* **187**, 197–211 (2004).
2. Manies, K. L., Harden, J. W., Bond-Lamberty, B. P. & O'Neill, K. P. Woody debris along an upland chronosequence in boreal Manitoba and its impact on long-term carbon storage. *Can. J. For. Res.* **35**, 472–482, <https://doi.org/10.1139/x04-179> (2005).
3. Guo, L. B., Bek, E. & Gifford, R. M. Woody debris in a 16-year old *Pinus radiata* plantation in Australia: Mass, carbon and nitrogen stocks, and turnover. *For. Ecol. Manag.* **228**, 145–151, <https://doi.org/10.1016/j.foreco.2006.02.043> (2006).
4. Müller-Using, S. & Bartsch, N. Decay dynamic of coarse and fine woody debris of a beech (*Fagus sylvatica* L.) forest in Central Germany. *Eur. J. For. Res.* **128**, 287–296, <https://doi.org/10.1007/s10342-009-0264-8> (2009).

5. Zalamea, M., González, G., Ping, C. L. & Michaelson, G. Soil organic matter dynamics under decaying wood in a subtropical wet forest: effect of tree species and decay stage. *Plant Soil* **296**, 173–185, <https://doi.org/10.1007/s11104-007-9307-4> (2007).
6. Preston, C. M., Trofymow, J. A. & Nault, J. R. Decomposition and change in N and organic composition of small-diameter Douglas-fir woody debris over 23 years. *Can. J. For. Res.* **42**, 1153–1167, <https://doi.org/10.1139/x2012-076> (2012).
7. Kirk, T. K. & Highley, T. L. Quantitative changes in structural components of conifer woods during decay by white- and brown-rot fungi. *Phytopathology* **63**, 1338–1342 (1973).
8. Green, F. I. & Highley, T. L. Mechanism of brown-rot decay: paradigm or paradox. *Int. Biodeterior. Biodegrad.* **39**, 113–124 (1997).
9. Mahajan, S., Jeremic, D., Goacher, R. E. & Master, E. R. Mode of coniferous wood decay by the white rot fungus *Phanerochaete carnosus* as elucidated by FTIR and ToF-SIMS. *Appl. Microbiol. Biotechnol.* **94**, 1303–1311, <https://doi.org/10.1007/s00253-011-3830-1> (2012).
10. Bailey, V. L., Smith, J. L. & Bolton, H. J. Fungal-to-bacterial ratios in soils investigated for enhanced C sequestration. *Soil Biol. Biochem.* **34**, 997–1007 (2002).
11. Six, J., Frey, S. D. & Thiet, R. K. & Batten, K. M. Bacterial and Fungal Contributions to Carbon Sequestration in Agroecosystems. *Soil Sci. Soc. Am. J.* **70**, 555, <https://doi.org/10.2136/sssaj2004.0347> (2006).
12. Sánchez, C. Lignocellulosic residues: biodegradation and bioconversion by fungi. *Biotechnol. Adv.* **27**, 185–194, <https://doi.org/10.1016/j.biotechadv.2008.11.001> (2009).
13. Sarkar, P., Bosneaga, E. & Auer, M. Plant cell walls throughout evolution: towards a molecular understanding of their design principles. *J. Exp. Bot.* **60**, 3615–3635, <https://doi.org/10.1093/jxb/erp245> (2009).
14. Harmon, M. E. *et al.* Ecology of coarse woody debris in temperate ecosystems. *Adv. Ecol. Res.* **15**, 133–302 (1986).
15. Martínez, Á. T. *et al.* Biodegradation of lignocellulosics: microbial, chemical, and enzymatic aspects of the fungal attack of lignin. *Int. Microbiol.* **8**, 195–204 (2005).
16. Pouska, V., Svoboda, M. & Lepšová, A. The diversity of wood-decaying fungi in relation to changing site conditions in an old-growth mountain spruce forest, Central Europe. *Eur. J. For. Res.* **129**, 219–231, <https://doi.org/10.1007/s10342-009-0324-0> (2010).
17. Leonowicz, A. *et al.* Biodegradation of Lignin by White Rot Fungi. *Fungal Genet. Biol.* **27**, 175–185 (1999).
18. Filley, T. R. *et al.* Lignin demethylation and polysaccharide decomposition in spruce sapwood degraded by brown rot fungi. *Org. Geochem.* **33**, 111–124 (2002).
19. Filley, T. R. Assessment of fungal wood decay by lignin analysis using tetramethyl- ammonium hydroxide (TMAH) and C-13-labeled TMAH thermochemolysis In *Wood deterioration and preservation: advances in our changing world* (eds. Goodell, B., Nicholas, D. D. & Schultz, T. P.) 119–139 (American Chemical Society, 2003).
20. Pandey, K. K. & Pitman, A. J. FTIR studies of the changes in wood chemistry following decay by brown-rot and white-rot fungi. *Int. Biodeterior. Biodegrad.* **52**, 151–160 (2003).
21. Filley, T. R., Nierop, K. G. J. & Wang, Y. The contribution of polyhydroxyl aromatic compounds to tetramethylammonium hydroxide lignin-based proxies. *Org. Geochem.* **37**, 711–727, <https://doi.org/10.1016/j.orggeochem.2006.01.005> (2006).
22. Guggenberger, G. & Kaiser, K. Dissolved organic matter in soil: challenging the paradigm of sorptive preservation. *Geoderma* **113**, 293–310, [https://doi.org/10.1016/s0016-7061\(02\)00366-x](https://doi.org/10.1016/s0016-7061(02)00366-x) (2003).
23. Lehmann, J. & Kleber, M. The contentious nature of soil organic matter. *Nature* **528**, 60–68, <https://doi.org/10.1038/nature16069> (2015).
24. Liang, C. & Balsler, T. C. Microbial production of recalcitrant organic matter in global soils: implications for productivity and climate policy. *Nat. Rev. Microbiol.* **9**, 75, <https://doi.org/10.1038/nrmicro2386-c1> (2011).
25. Mambelli, S., Bird, J. A., Gleixner, G., Dawson, T. E. & Torn, M. S. Relative contribution of foliar and fine root pine litter to the molecular composition of soil organic matter after *in situ* degradation. *Org. Geochem.* **42**, 1099–1108, <https://doi.org/10.1016/j.orggeochem.2011.06.008> (2011).
26. Miltner, A., Bombach, P., Schmidt-Brücken, B. & Kästner, M. SOM genesis: microbial biomass as a significant source. *Biogeochemistry* **111**, 41–55, <https://doi.org/10.1007/s10533-011-9658-z> (2012).
27. Ludwig, M. *et al.* Microbial contribution to SOM quantity and quality in density fractions of temperate arable soils. *Soil Biol. Biochem.* **81**, 311–322, <https://doi.org/10.1016/j.soilbio.2014.12.002> (2015).
28. Sollins, P. *et al.* Organic C and N stabilization in a forest soil: Evidence from sequential density fractionation. *Soil Biol. Biochem.* **38**, 3313–3324, <https://doi.org/10.1016/j.soilbio.2006.04.014> (2006).
29. Kleber, M. What is recalcitrant soil organic matter? *Environ. Chem.* **7**, 320–332, <https://doi.org/10.1071/en10006> (2010).
30. Kuzyakov, Y. & Bol, R. Sources and mechanisms of priming effect induced in two grassland soils amended with slurry and sugar. *Soil Biol. Biochem.* **38**, 747–758, <https://doi.org/10.1016/j.soilbio.2005.06.025> (2006).
31. Waldrop, M. P. & Firestone, M. K. Microbial community utilization of recalcitrant and simple carbon compounds: impact of oak-woodland plant communities. *Oecologia* **138**, 275–284, <https://doi.org/10.1007/s00442-003-1419-9> (2004).
32. Kuzyakov, Y. Priming effects: Interactions between living and dead organic matter. *Soil Biol. Biochem.* **42**, 1363–1371, <https://doi.org/10.1016/j.soilbio.2010.04.003> (2010).
33. Fanin, N., Fromin, N. & Bertrand, I. Functional breadth and home-field advantage generate functional differences among soil microbial decomposers. *Ecology* **97**, 1023–1037 (2016).
34. Keiluweit, M. *et al.* Mineral protection of soil carbon counteracted by root exudates. *Nat. Clim. Chang.* **5**, 588–595, <https://doi.org/10.1038/nclimate2580> (2015).
35. Torsvik, V. & Øvreås, L. Microbial diversity and function in soil: from genes to ecosystems. *Curr. Opin. Microbiol.* **5**, 240–245 (2002).
36. Nannipieri, P. *et al.* Microbial diversity and soil functions. *Eur. J. Soil Sci.* **54**, 655–670, <https://doi.org/10.1046/j.1365-2389.2003.00556.x> (2003).
37. Rajala, T., Peltoniemi, M., Hantula, J., Mäkipää, R. & Pennanen, T. RNA reveals a succession of active fungi during the decay of Norway spruce logs. *Fungal Ecol.* **4**, 437–448, <https://doi.org/10.1016/j.funeco.2011.05.005> (2011).
38. Lundin, D. *et al.* Which sequencing depth is sufficient to describe patterns in bacterial alpha- and beta-diversity? *Environ. Microbiol. Rep.* **4**, 367–372, <https://doi.org/10.1111/j.1758-2229.2012.00345.x> (2012).
39. Bastida, F., Selevsek, N., Torres, I. F., Hernandez, T. & Garcia, C. Soil restoration with organic amendments: linking cellular functionality and ecosystem processes. *Sci. Rep.* **5**, 15550, <https://doi.org/10.1038/srep15550> (2015).
40. Mau, R. L. *et al.* Linking soil bacterial biodiversity and soil carbon stability. *ISME J.* **9**, 1477–1480, <https://doi.org/10.1038/ismej.2014.205> (2015).
41. Glaser, B., Millar, N. & Blum, H. Sequestration and turnover of bacterial- and fungal-derived carbon in a temperate grassland soil under long-term elevated atmospheric pCO₂. *Glob. Chang. Biol.* **12**, 1521–1531, <https://doi.org/10.1111/j.1365-2486.2006.01186.x> (2006).
42. Derrien, D. & Amelung, W. Computing the mean residence time of soil carbon fractions using stable isotopes: impacts of the model framework. *Eur. J. Soil Sci.* **62**, 237–252, <https://doi.org/10.1111/j.1365-2389.2010.01333.x> (2011).
43. Amelung, W., Miltner, A., Zhang, X. & Zech, W. Fate of microbial residues during litter decomposition as affected by minerals. *Soil Sci. Plant Nutr.* **166**, 598–606 (2001).
44. Glaser, B., Turrión, M.-B. & Alef, K. Amino sugars and muramic acid—biomarkers for soil microbial community structure analysis. *Soil Biol. Biochem.* **36**, 399–407, <https://doi.org/10.1016/j.soilbio.2003.10.013> (2004).
45. Bai, Z., Bodé, S., Huygens, D., Zhang, X. D. & Boeckx, P. Kinetics of amino sugar formation from organic residues of different quality. *Soil Biol. Biochem.* **57**, 814–821, <https://doi.org/10.1016/j.soilbio.2012.08.006> (2013).

46. Farkaš, N. Biosynthesis of cell walls of fungi. *Microbiol. Rev.* **43**, 117–144 (1979).
47. Scheffers, D. J. & Pinho, M. G. Bacterial cell wall synthesis: new insights from localization studies. *Microbiol. Mol. Biol. Rev.* **69**, 585–607, <https://doi.org/10.1128/MMBR.69.4.585-607.2005> (2005).
48. Dai, X. Y., Ping, C. L., Hines, M. E., Zhang, X. D. & Zech, W. Amino sugars in arctic soils. *Commun. Soil Sci. Plant Anal.* **33**, 789–805, <https://doi.org/10.1081/css-120003066> (2002).
49. Pronk, G. J., Heister, K. & Kögel-Knabner, I. Amino sugars reflect microbial residues as affected by clay mineral composition of artificial soils. *Org. Geochem.* **83–84**, 109–113, <https://doi.org/10.1016/j.orggeochem.2015.03.007> (2015).
50. Spears, J. D., Holub, S. M., Harmon, M. E. & Lajtha, K. The influence of decomposing logs on soil biology and nutrient cycling in an old-growth mixed coniferous forest in Oregon, USA. *Can. J. For. Res.* **33**, 2193–2201, <https://doi.org/10.1139/x03-148> (2003).
51. Ma, Y., Filley, T. R., Szlavetz, K. & McCormick, M. K. Controls on wood and leaf litter incorporation into soil fractions in forests at different successional stages. *Soil Biol. Biochem.* **69**, 212–222, <https://doi.org/10.1016/j.soilbio.2013.10.043> (2014).
52. Goldin, S. R. & Hutchinson, M. F. Coarse woody debris modifies surface soils of degraded temperate eucalypt woodlands. *Plant Soil* **370**, 461–469, <https://doi.org/10.1007/s11104-013-1642-z> (2013).
53. Spears, J. D. H. & Lajtha, K. The imprint of coarse woody debris on soil chemistry in the western Oregon Cascades. *Biogeochemistry* **71**, 163–175 (2005).
54. Marra, J. L. & Edmonds, R. L. Coarse woody debris and forest floor respiration in an old-growth coniferous forest on the Olympic Peninsula, Washington, USA. *Can. J. For. Res.* **24**, 1811–1817 (1994).
55. Rajala, T., Peltoniemi, M., Pennanen, T. & Mäkipää, R. Fungal community dynamics in relation to substrate quality of decaying Norway spruce (*Picea abies* [L.] Karst.) logs in boreal forests. *FEMS Microbiol. Ecol.* **81**, 494–505, <https://doi.org/10.1111/j.1574-6941.2012.01376.x> (2012).
56. Hart, S. C. Nitrogen transformations in fallen tree boles and mineral soil of an old-growth forest. *Ecology* **80**, 1385–1394 (1999).
57. Means, J. E., MacMillan, P. C. & Cromack, K. J. Biomass and nutrient content of Douglas-fir logs and other detrital pools in an old-growth forest, Oregon, USA. *Can. J. For. Res.* **22**, 1536–1546 (1992).
58. Strukelj, M., Brais, S., Quideau, S. & Oh, S.-W. Chemical transformations of deadwood and foliar litter of mixed boreal species during decomposition. *Can. J. For. Res.* **42**, 772–788, <https://doi.org/10.1139/x2012-027> (2012).
59. Büttler, R., Patty, L., Le Bayon, R.-C., Guenat, C. & Schlaepfer, R. Log decay of *Picea abies* in the Swiss Jura Mountains of central Europe. *For. Ecol. Manag.* **242**, 791–799, <https://doi.org/10.1016/j.foreco.2007.02.017> (2007).
60. Homyak, P. M., Yanai, R. D., Burns, D. A., Briggs, R. D. & Germain, R. H. Nitrogen immobilization by wood-chip application: Protecting water quality in a northern hardwood forest. *For. Ecol. Manag.* **255**, 2589–2601, <https://doi.org/10.1016/j.foreco.2008.01.018> (2008).
61. Weißhaupt, P., Pritzkow, W. & Noll, M. Nitrogen metabolism of wood decomposing basidiomycetes and their interaction with diazotrophs as revealed by IRMS. *Int. J. Mass Spectrom.* **307**, 225–231, <https://doi.org/10.1016/j.ijms.2010.12.011> (2011).
62. Lombardi, F. *et al.* Investigating biochemical processes to assess deadwood decay of beech and silver fir in Mediterranean mountain forests. *Ann. For. Sci.* **70**, 101–111, <https://doi.org/10.1007/s13595-012-0230-3> (2013).
63. Machuca, A. & Ferraz, A. Hydrolytic and oxidative enzymes produced by white- and brown-rot fungi during *Eucalyptus grandis* decay in solid medium. *Enzyme Microb. Technol.* **29**, 386–391 (2001).
64. del Río, J. C., Gutiérrez, A., Martínez, M. J. & Martínez, A. T. Py-GC/MS study of *Eucalyptus globulus* wood treated with different fungi. *J. Anal. Appl. Pyrolysis* **58–59**, 441–452 (2001).
65. Jurgensen, M. F., Larsen, M. J., Wolosiewicz, M. & Harvey, A. E. A comparison of dinitrogen fixation rates in wood litter decayed by white-rot and brown-rot fungi. *Plant Soil* **115**, 117–122 (1989).
66. Blagodatskaya, E. V., Blagodatsky, S. A., Anderson, T. H. & Kuzyakov, Y. Priming effects in Chernozem induced by glucose and N in relation to microbial growth strategies. *Appl. Soil Ecol.* **37**, 95–105, <https://doi.org/10.1016/j.apsoil.2007.05.002> (2007).
67. Qiu, Q., Wu, L., Ouyang, Z., Li, B. & Xu, Y. Different effects of plant-derived dissolved organic matter (DOM) and urea on the priming of soil organic carbon. *Environ. Sci. Process Impacts* **18**, 330–341, <https://doi.org/10.1039/c5em00446b> (2016).
68. Cerli, C. *et al.* Changes in humic substances along an age sequence of Norway spruce stands planted on former agricultural land. *Org. Geochem.* **39**, 1269–1280, <https://doi.org/10.1016/j.orggeochem.2008.06.001> (2008).
69. Dill, I., Salnikow, J. & Kraepeli, G. Hydroxyproline-rich protein material in wood and lignin of fagus sylvatica. *Appl. Environ. Microb.* **48**, 1259–1261 (1984).
70. Blanchette, R. A. Delignification by wood-decay fungi. *Annu. Rev. Phytopathol.* **29**, 381–398 (1991).
71. Tuor, U., Winterhalter, K. & Fiechter, A. Enzymes of white-rot fungi involved in lignin degradation and ecological determinants for wood decay. *J. Biotechnol.* **41**, 1–17 (1995).
72. McColl, J. G. & Powers, R. F. Decomposition of small diameter woody debris of red fir determined by nuclear magnetic resonance. *Commun. Soil Sci. Plant Anal.* **29**, 2691–2704, <https://doi.org/10.1080/00103629809370144> (1998).
73. Larsen, M. J. N₂ fixation associated with wood decayed by some common fungi in western Montana. *Can. J. For. Res.* **8**, 341–345 (1978).
74. Eastwood, D. C. *et al.* The plant cell wall-decomposing machinery underlies the functional diversity of forest fungi. *Science* **333**, 762–765, <https://doi.org/10.1126/science.1205411> (2011).
75. Jiao, Y. *et al.* Different progress of log decay on forest soil organic carbon and total nitrogen in Changbai Mountain. *Chin. J. Soil Sci.* **46**, 1096–1102 (in Chinese) (2015).
76. Kohzu, A. *et al.* Dynamics of ¹³C natural abundance in wood decomposing fungi and their ecophysiological implications. *Soil Biol. Biochem.* **37**, 1598–1607, <https://doi.org/10.1016/j.soilbio.2005.01.021> (2005).
77. Fukasawa, Y., Takahashi, K., Arikawa, T., Hattori, T. & Maekawa, N. Fungal wood decomposer activities influence community structures of myxomycetes and bryophytes on coarse woody debris. *Fungal Ecol.* **14**, 44–52, <https://doi.org/10.1016/j.funeco.2014.11.003> (2015).
78. Parihar, J., Tiwari, C. K., Ayachi, A. & Verma, R. K. Biodegradation of cellulose by wood decaying fungi. *J. Appl. Sci. Environ. Sanit.* **7**, 209–214 (2012).
79. Holland, E. A. & Coleman, D. C. Litter placement effects on microbial and organic-matter dynamics in an agroecosystem. *Ecology* **68**, 425–433 (1987).
80. Strickland, M. S. & Rousk, J. Considering fungal:bacterial dominance in soils – Methods, controls, and ecosystem implications. *Soil Biol. Biochem.* **42**, 1385–1395, <https://doi.org/10.1016/j.soilbio.2010.05.007> (2010).
81. Trivedi, P., Anderson, I. C. & Singh, B. K. Microbial modulators of soil carbon storage: integrating genomic and metabolic knowledge for global prediction. *Trends Microbiol.* **21**, 641–651, <https://doi.org/10.1016/j.tim.2013.09.005> (2013).
82. Helfrich, M., Ludwig, B., Thoms, C., Gleixner, G. & Flessa, H. The role of soil fungi and bacteria in plant litter decomposition and macroaggregate formation determined using phospholipid fatty acids. *Appl. Soil Ecol.* **96**, 261–264, <https://doi.org/10.1016/j.apsoil.2015.08.023> (2015).
83. Schneider, T. *et al.* Who is who in litter decomposition? Metaproteomics reveals major microbial players and their biogeochemical functions. *ISME J.* **6**, 1749–1762, <https://doi.org/10.1038/ismej.2012.11> (2012).
84. Yuan, Z. *et al.* Scale specific determinants of tree diversity in an old growth temperate forest in China. *Basic Appl. Ecol.* **12**, 488–495, <https://doi.org/10.1016/j.baae.2011.07.008> (2011).
85. Han, C. L. *et al.* Properties and taxonomy of soils developed from volcano ejecta in Changbai mountains. *ACTA Pedol. Sin.* **50**, 1061–1070 (2013).

86. Dai, Y. C. Polypore diversity in China with an annotated checklist of Chinese polypores. *Mycoscience* **53**, 49–80, <https://doi.org/10.1007/s10267-011-0134-3> (2012).
87. Dai, Y. C., Cui, B. K., Yuan, H. S. & Li, B. D. Pathogenic wood-decaying fungi in China. *For. Pathol.* **37**, 105–120 (2007).
88. Liu, N. *et al.* Impacts of long-term inorganic and organic fertilization on lignin in a Mollisol. *J. Soil. Sediment.* **10**, 1466–1474, <https://doi.org/10.1007/s11368-010-0298-z> (2010).
89. Zhang, X. D. & Amelung, W. Gas chromatographic determination of muramic acid, glucosamine, mannosamine, and galactosamine in soils. *Soil Biol. Biochem.* **28**, 1201–1206 (1996).
90. Liang, C., Read, H. W. & Balser, T. C. GC-based detection of aldonitrile acetate derivatized glucosamine and muramic acid for microbial residue determination in soil. *J. Vis. Exp.*, E3767, <https://doi.org/10.3791/3767> (2012).
91. Appuhn, A. & Joergensen, R. Microbial colonisation of roots as a function of plant species. *Soil Biol. Biochem.* **38**, 1040–1051, <https://doi.org/10.1016/j.soilbio.2005.09.002> (2006).
92. Engelking, B., Flessa, H. & Joergensen, R. G. Shifts in amino sugar and ergosterol contents after addition of sucrose and cellulose to soil. *Soil Biol. Biochem.* **39**, 2111–2118, <https://doi.org/10.1016/j.soilbio.2007.03.020> (2007).
93. White, D. C. & Findlay, R. H. Biochemical markers for measurement of predation effects on the biomass, community structure, nutritional status, and metabolic activity of microbial biofilms. *Hydrobiologia* **159**, 119–132 (1988).
94. Xu, B., Feng, X. & Burdine, R. D. Categorical data analysis in experimental biology. *Dev. Biol.* **348**, 3–11, <https://doi.org/10.1016/j.ydbio.2010.08.018> (2010).

Acknowledgements

The authors would like to acknowledge funding received from the National Natural Science Foundation of China (31670506, 41571237, 41630862), and “China Soil Microbiome Initiative: Function and regulation of soil - microbial systems” of the Chinese Academy of Sciences (XDB15010303). We also appreciate the valuable assistance provided by Timothy R. Filley.

Author Contributions

Z.B. designed and performed the research, analyzed the data and wrote the paper. Y.D. and J.Y. helped in the collection of samples. H.Y., Q.M. and W.Y. provided good advice for the paper.

Additional Information

Supplementary information accompanies this paper at <https://doi.org/10.1038/s41598-017-14181-7>.

Competing Interests: The authors declare that they have no competing interests.

Publisher's note: Springer Nature remains neutral with regard to jurisdictional claims in published maps and institutional affiliations.



Open Access This article is licensed under a Creative Commons Attribution 4.0 International License, which permits use, sharing, adaptation, distribution and reproduction in any medium or format, as long as you give appropriate credit to the original author(s) and the source, provide a link to the Creative Commons license, and indicate if changes were made. The images or other third party material in this article are included in the article's Creative Commons license, unless indicated otherwise in a credit line to the material. If material is not included in the article's Creative Commons license and your intended use is not permitted by statutory regulation or exceeds the permitted use, you will need to obtain permission directly from the copyright holder. To view a copy of this license, visit <http://creativecommons.org/licenses/by/4.0/>.

© The Author(s) 2017